

Wakes of Four Complex Bodies of Revolution at Zero Angle of Attack

Veysel Atli*

Istanbul Technical University, Istanbul, Turkey

The wakes of four complex bodies of revolution were investigated experimentally with a constant-temperature hot-wire anemometer. All tests were performed at a low Mach number ($M_\infty \approx 0.1$) and zero angle of attack. Mean and turbulence velocity profiles were obtained along and across the wakes. The structure of the axisymmetric wake and the effects of the geometric differences of the models on their wakes were investigated.

Nomenclature

d	= maximum diameter of the model
l	= total length of the model
l/d	= fineness ratio of the model
M_∞	= Mach number
Re_d	= $[(V_\infty d)/\nu]$ Reynolds number based on the freestream conditions and the maximum body diameter
V_∞	= freestream velocity
\bar{V}	= mean velocity
$(\bar{V}_{x\bar{x}})$	= mean velocity in the x direction on the wake centerline
$(V_{x\bar{x}})_{\max}$	= maximum reverse flow velocity in the x direction on the wake centerline in the recirculation region
$(v_x'^2)^{1/2}$	= rms turbulence in the x direction
v_0	= $[(v_x'^2)^{1/2}/V_\infty]$ rms turbulence in the x direction, normalized with V_∞
$(v_x'^2)^{1/2}$	= rms turbulence in the x direction on the wake centerline
v_1	= $[(v_x'^2)^{1/2}/V_\infty]$ rms turbulence in the x direction, on the centerline of the wake, normalized with V_∞
v_2	= $[(v_x'^2)^{1/2}/ \bar{V}_{x\bar{x}}]$ rms turbulence in the x direction, on the centerline of the wake, normalized with $ \bar{V}_{x\bar{x}} $
x	= distance from the base of the model in the freestream direction
x_{sp}	= length of the recirculation region (distance from the base to the near stagnation point)
α	= angle of attack
ν	= kinematic viscosity of air

Subscripts

\bar{x}	= on the wake centerline
max	= maximum value
x	= in the x direction
∞	= freestream conditions

I. Introduction

THE flow separation aft of a blunt-based body of revolution at zero angle of attack creates an axisymmetric wake just behind the body. This region strongly affects the aerodynamic characteristics of the body, and it is therefore desirable to investigate this wake in detail.

The wake is the most complex part of the flowfield and may be divided into the recirculation region, the free-stagnation

point, and the far-wake region. The structure of the wake depends on many parameters such as the geometric form of the body, Reynolds number, and Mach number.

Many experimental works already have been devoted to this problem because of its practical importance. Delery and Sirieix¹ outlined the problem and gave a large list of the literature. References 2–7 represent only some of the recent experimental works. Calvert² made mean velocity, turbulence, and static pressure measurements in the wakes of several cones (including a disk and a cylinder) with different cone angles and showed that the wakes of these types of bodies at zero angle of attack are all essentially similar with the form of the near-wake in a closed bubble. Merz et al.³ investigated the effect of Mach number on the turbulent near-wake of a cylindrical blunt-based body at the entire subsonic Mach number range by using a special wind tunnel and a standard Prandtl pitot-static probe. Gai and Patil,⁴ Gai and Kapoor,⁵ and Porteiro et al.⁷ have tested some techniques to reduce the base drag by modifying the wake. However, these and other works generally have considered simple bodies of revolution such as cones or ellipsoidal-nosed cylinders. Moreover, the detailed structure of the wake (especially the turbulence structure of the near-wake region) and the effects of body geometric parameters on it are not obvious, even for the simple-type bodies of revolution.

The purpose of this work is to extend our knowledge about the structure of the axisymmetric wake and the effect of the geometric form of the body on it. For this purpose, the wakes of four complex bodies of revolution at zero angle of attack and at a low subsonic velocity were tested by using a constant-temperature hot-wire anemometer. The mean and turbulence velocity profiles both along and across the wake were obtained. Turbulence is treated as the time-averaged rms fluctuating velocities in the present work.

Descriptions of the models and the experimental techniques are presented in Sec. II. The results and discussion are given in Sec. III. The conclusion is presented in Sec. IV. A more detailed description of the current work can be found in Ref. 8.

II. Description of the Models and Experimental Technique

The models used for tests are shown in Fig. 1. All of the models had the same fineness ratio $l/d = 7.5$. The geometric forms of the models were chosen in such a way as to permit the observation of the effects of the certain geometric differences on the structure of the wake. Whereas the first model is a constant-diameter cylinder, the last one has a geometric shape of a particular missile, with junctions, gaps, and flat nose, consisting of cylindrical and conical parts. The other models have the forms in-between the first and last one, so that the second one is a hemiellipsoid nose-cylinder and the third one a truncated cone nose-cylinder.

Received Dec. 19, 1986; revision received Feb. 7, 1988. Copyright © American Institute of Aeronautics and Astronautics, Inc., 1989. All rights reserved.

*Associate Professor, Doctor, Faculty of Aeronautics and Astronautics.

All of the tests were conducted at zero angle of attack, $\alpha = 0$ deg, in an open-circuit, low-speed wind tunnel with a closed test section of $30 \times 30 \times 100$ cm. The freestream velocity V_∞ was 25 m/s with the freestream turbulence intensity $(\overline{v_x'^2})^{1/2}/V_\infty = 0.5\%$. The Reynolds number $Re_d (= V_\infty d/\nu)$ was 1.16×10^5 . A DISA 55M10 hot-wire anemometer (CTA) with a 55D25 auxiliary unit, 55D31 digital voltmeter, 55D35 rms unit, 55D15 linearizer (with 52A40 power supply); a traversing mechanism with 52C01 external stepper motor, 52B01 sweep drive unit; a standard-type hot-wire probe (P01) of DISA; and two X-Y recorders (for recording the mean velocity and turbulence velocity outputs of the anemometer) were used to measure the wake velocities. In these tests, for each model, first a traverse along the centerline of the wake was made, followed by the cross traverses at several longitudinal stations. Hence, the mean and turbulence velocity profiles both along and across the wake were obtained. These profiles were analyzed in detail. The positional accuracy of the probe traverse was ± 0.1 mm.

III. Results and Discussion

The mean velocity distributions along the centerline of the wake for all the models are presented in Fig. 2. The length of the recirculation region is about 1.1 times the maximum body diameter ($x_{sp} = 1.1d$) for all of the models. Reverse flow on the centerline of the wake in the recirculation region reaches its maximum velocity at a distance from the base of about 60% of the length of the recirculation region. The maximum velocity of the reverse flow on the centerline of the wake $(\overline{V_{x\epsilon}})_{\max}$ ranges from 25 to 35% of the freestream velocity V_∞ (25% for model 2 and 35% for model 4), depending on the model configuration. It seems that the geometric complexity at the rear part of the body causes an increase in the reverse-flow velocity. As seen from Fig. 3, the mean velocity distributions along the centerline of the wake in the recirculation region for all of the models are consistent with those of Merz et al.³ obtained experimentally for a cylinder in the entire subsonic Mach number range.

The velocity fluctuations (turbulence velocity) on the centerline of the wake were expressed in terms of freestream velocity and local mean velocity as $v_1 = (\overline{v_x'^2})^{1/2}/V_\infty$ and $v_2 = (\overline{v_x'^2})^{1/2}/|\overline{V_{x\epsilon}}|$, respectively. Figure 4 shows the variation of v_1 along the centerline of the wake for all of the models. As seen from this figure, v_1 attains its maximum value before the midpoint of the distance between the base and free-stagnation point and just after the free-stagnation point. It also receives its minimum values near the base and near the free-stagnation point. Figure 5 shows the variations of v_2 along the wake centerline for all of the models. As shown in this figure, v_2 has two maximum points: one near the base and the other near the free-stagnation point. It has a minimum point near the midpoint of the distance between the base and the free-stagnation point. It decreases continuously in the far-wake region along the centerline of the wake. Since v_2 expresses the local unsteadiness of flow, it is observed from this figure that the wake near the base and the free-stagnation point is less steady than the rest of the wake. The variations of v_1 and v_2 obtained in this work are similar to those obtained by Calvert² for cones, plate, and cylinder.

Although the original hot-wire signal has no directional information, flow reversal in the near-wake may be inferred from the abrupt change in the magnitude of the signal at the edge of this region. Figure 6 shows flow reversal to be stronger in the near-wake of model 4 than in other configurations. This fact may be because of the diverging conical shape of the rear part of model 4. The very broad wake region at large x/d for model 1 may be attributed to flow separation at the sharp leading edge of the body.

Figure 7 shows the turbulence $[v_0 = (\overline{v_x'^2})^{1/2}/V_\infty]$ profiles across the wake at several longitudinal stations for all of the models. As shown in this figure, the maximum turbulence in the wake takes place on an approximately cylindrical surface

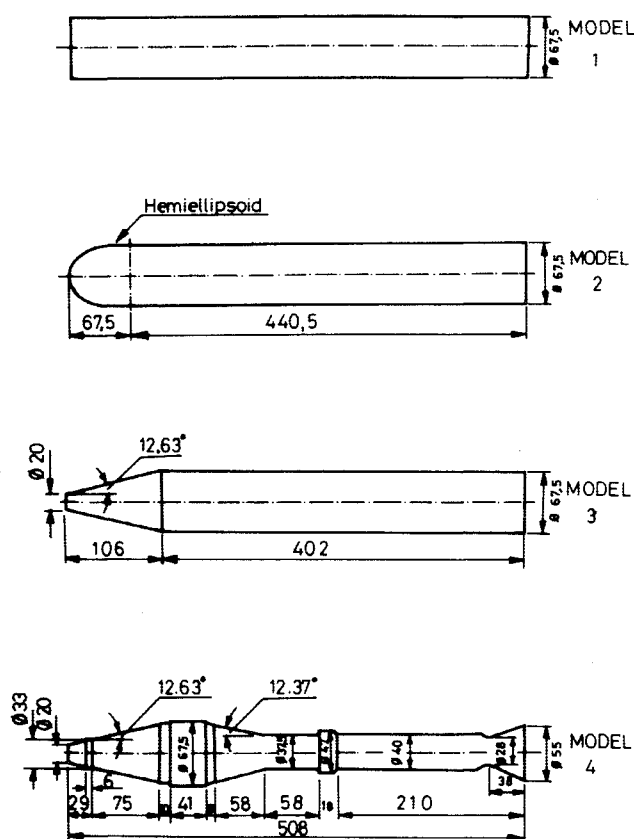


Fig. 1 Models used for tests (all dimensions in mm).

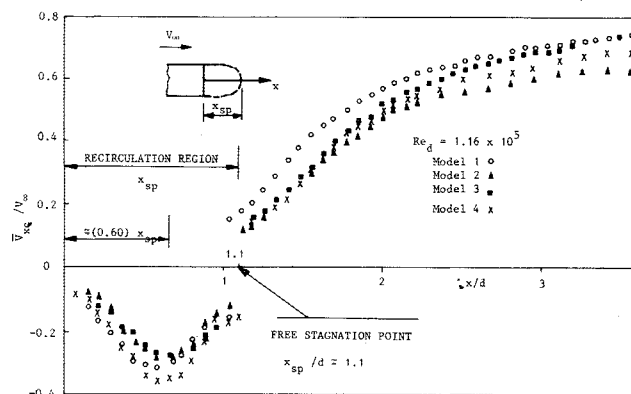


Fig. 2 Mean velocity distribution along the centerline of the wake for all of the models.

around the wake centerline, which extends toward the free-stagnation point where it diverges and reaches its highest value ($v_0 \approx 15\%$) on a circle around the free-stagnation point with a radius of 0.6 times the maximum radius of the body. One might also identify another maximum turbulence surface in the recirculation region. This conical surface converges from the base toward the free-stagnation point. It is clear that the geometric complexity at the rear part of the body (as model 4) increases the turbulence in the recirculation region, whereas the flow separation at the front part of the body (as model 1) increases the turbulence at the edge of the wake. This fact may be important from a practical point of view. For instance, the increase in turbulence in the recirculation region can increase the base pressure due to the enhanced mixing between the recirculation and the outer regions.

The mean and turbulence velocity profiles across the wake for model 4 are plotted together in Fig. 8. The points that were observed from Figs. 6 and 7 may be seen more clearly in Fig. 8. In addition, the maximum points on the turbulence

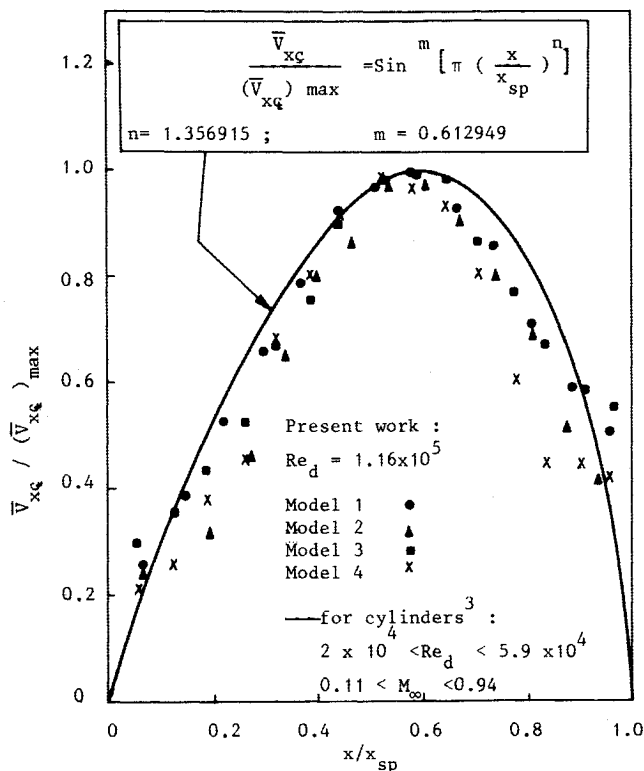


Fig. 3 Mean velocity distribution along the centerline of the wake in the recirculation region for all of the models: —, result of Merz et al.³ for cylinders.

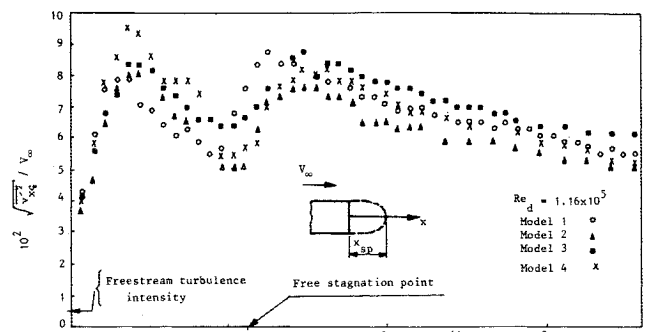


Fig. 4 Longitudinal variations of velocity fluctuations in terms of percentage of freestream velocity for all of the models.

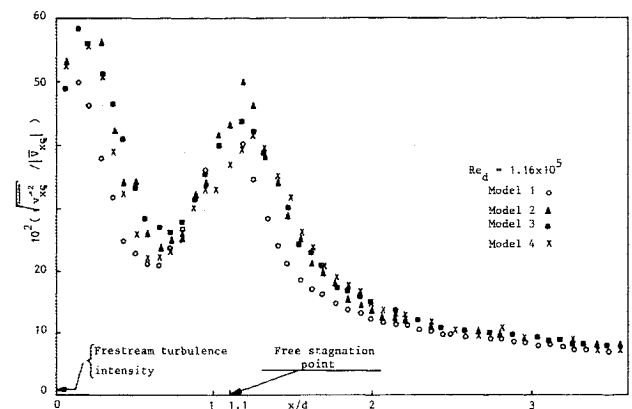


Fig. 5 Longitudinal variations of velocity fluctuations in terms of percentage of the local mean velocity on the wake centerline for all of the models.

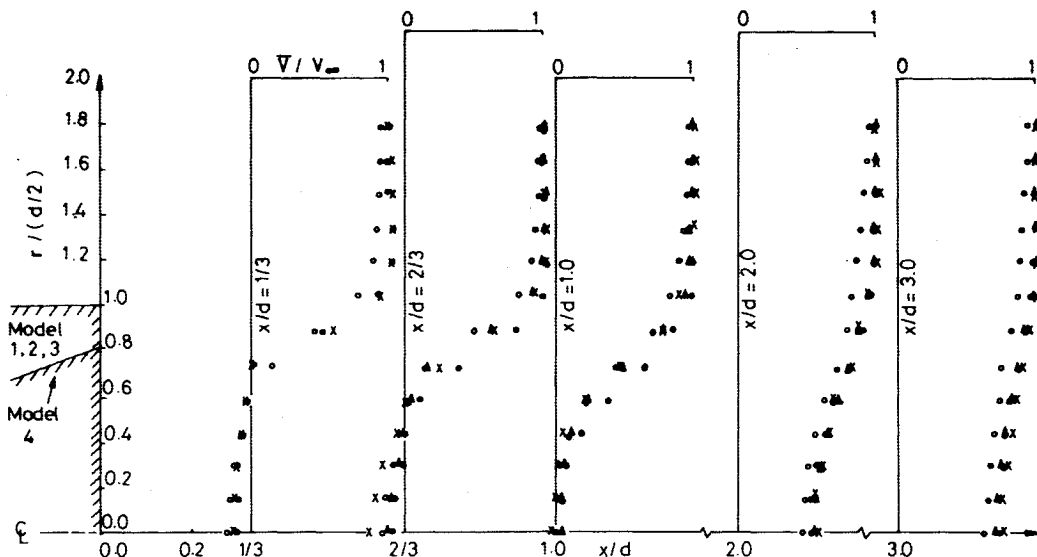


Fig. 6 Mean velocity profiles across the wake at several stations for all of the models: ○, model 1; ●, model 2; △, model 3; ×, model 4.

profiles correspond to the points on which the mean velocity gradient has the maximum values.

IV. Conclusions

The wakes of four complex bodies of revolution were investigated experimentally at a low Mach number ($M_\infty \approx 0.1$) and zero angle of attack by using a constant-temperature hot-wire anemometer. The effect of body shape in the wake structure was examined, and the following observations were made:

1) All wakes have a recirculation region between the base and the free-stagnation point and a far-wake region after the

free-stagnation point.

2) The length of the recirculation region is about 1.1 times the maximum body diameter ($x_{sp} \approx 1.1d$) for all of the models.

3) The reverse flow on the centerline of the wake in the recirculation region reaches its maximum velocity at a distance from the base of about 60% of the length of the recirculation region. The geometric complexity at the rear part of the body causes an increase in the reverse-flow velocity; thus, the maximum velocity of the reverse flow on the centerline of the wake ranges from 25 to 35% of the freestream velocity (25% for model 2 and 35% for model 4).

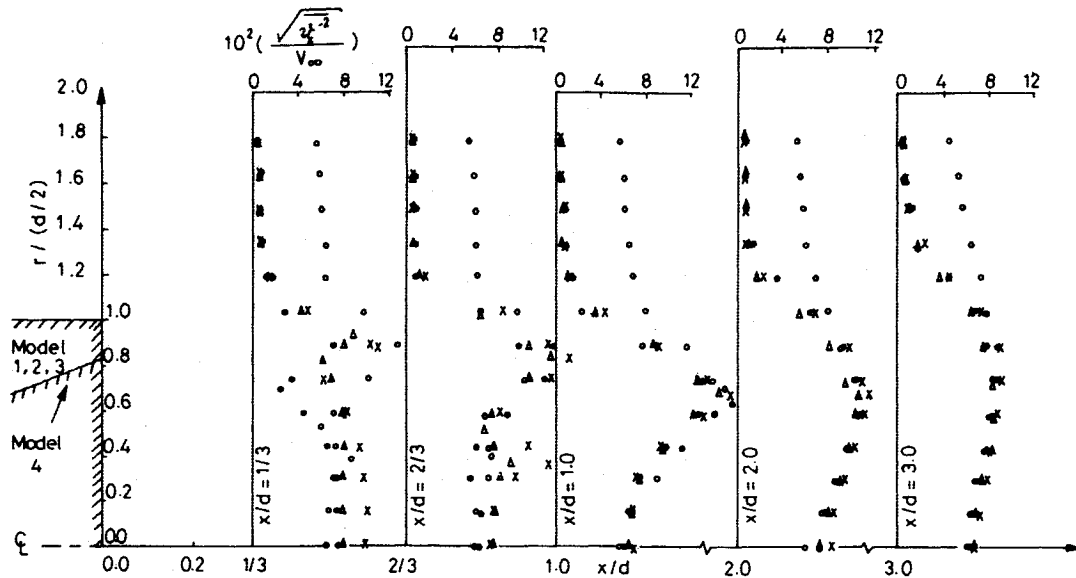


Fig. 7 Turbulence profiles across the wake at several stations for all of the models: \circ , model 1; \bullet , model 2; Δ , model 3; \times , model 4.

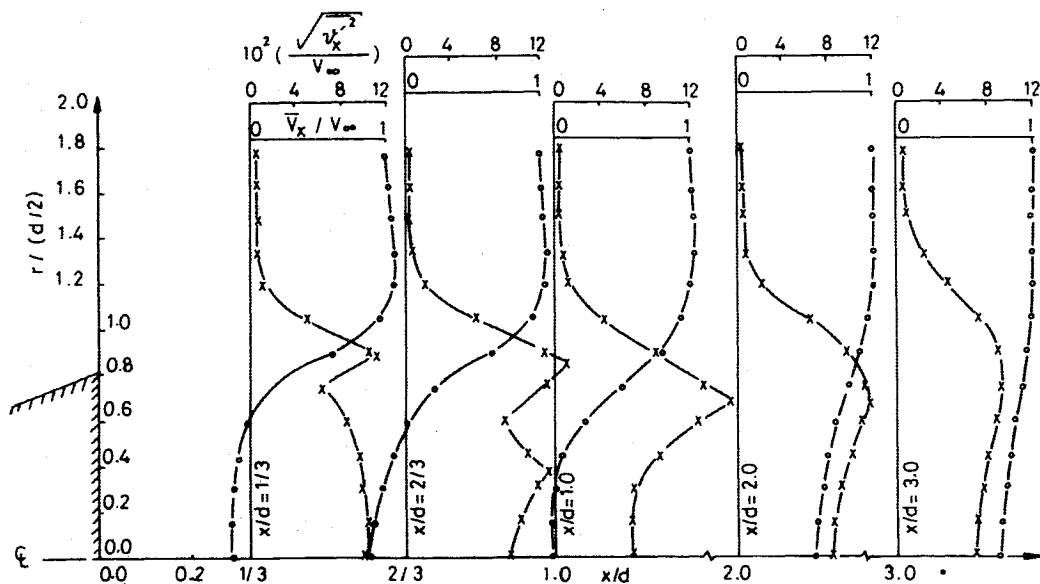


Fig. 8 Mean velocity and turbulence profiles across the wake at several stations for model 4: \circ , mean velocity profiles; \times , turbulence profiles.

4) Two local maxima of the ratio of the rms of turbulence on the wake centerline to the freestream velocity lie before the midpoint of the distance between the base and the free-stagnation point and just after the free-stagnation point. The minimum values are near the base and the free-stagnation point.

5) The ratio of the rms of turbulence on the wake centerline to the local mean velocity has two maxima: one near the base and the other near the free-stagnation point. This means that the wake near the base and the free-stagnation point is less steady than the rest of the wake.

6) The mean velocity profiles across the wake for the near-wake region have peak values greater than the freestream velocity just before leaving the wake (in the free-shear layer) unlike the mean velocity profiles of the far-wake region.

7) The geometric complexity at the rear part of the body

affects the recirculation region, as evidenced by an increase in the mean velocity and turbulence, whereas large flow separation at the front part of the body affects the wake outside the recirculation region, making the wake larger and increasing turbulence but decreasing the mean velocity at the edge of the wake.

8) There is an approximately cylindrical surface around the wake centerline on which turbulence reaches its highest value in every cross section of the wake. Another maximum turbulence surface might be identified in the recirculation region. This conical surface converges from the base toward the free-stagnation point.

9) The maximum points on the turbulence profiles across the wake correspond to the points on which the mean velocity gradient has the maximum values.

Acknowledgment

The author wishes to acknowledge Professors M. Z. Erim, J. F. Wendt, and Y. Tulunay for their support; N. Z. Orbay for his valuable help in the hot-wire measurements; and the referee of the *AIAA Journal* for his recommendations, which improved the paper.

References

- ¹Delery, J. and Sirieix, M., "Ecoulements de Culot," AGARD-LS-99, March 1979, pp. 6.1-6.78.
- ²Calvert, J. R., "Experiments on the Low-Speed Flow Past Cones," *Journal of Fluid Mechanics*, Vol. 27, Pt. 2, Feb. 1967, pp. 273-289.
- ³Merz, R. A., Page, R. H., and Przirembel, C. E. G., "Subsonic Axisymmetric Near-Wake Studies," *AIAA Journal*, Vol. 16, July 1978, pp. 656-662.

⁴Gai, S. L. and Patil, S. R., "Subsonic Axisymmetric Base Flow Experiments with Base Modifications," *Journal of Spacecraft and Rockets*, Vol. 17, No. 1, Jan.-Feb. 1980, pp. 42-46.

⁵Gai, S. L. and Kapoor, K., "Jet Effects on Near Wake of an Axisymmetric Bluff Body," *Journal of Spacecraft and Rockets*, Vol. 18, No. 6, Nov.-Dec. 1981, pp. 540-544.

⁶Kapoor, K., "Effect of Radial Fins on Base Drag of an Axisymmetric Body at Low Speeds," *Journal of Spacecraft and Rockets*, Vol. 19, No. 1, Jan.-Feb. 1982, pp. 89-92.

⁷Porteiro, J. L. F., Przirembel, C. E. G., and Page, R. H., "Modification of Subsonic Wakes Using Boundary Layer and Base Mass Transfer," *AIAA Journal*, Vol. 21, May 1983, pp. 665-670.

⁸Atli, V., "Theoretical and Experimental Investigation on the Aerodynamic Characteristics of Some Bodies of Revolution Used in Aeronautics," Ph.D. Dissertation, Istanbul Technical Univ., Faculty of Mechanical Engineering, Dept. of Aeronautical Engineering, Istanbul, Turkey, 1984.

Recommended Reading from the AIAA Progress in Astronautics and Aeronautics Series . . .



Dynamics of Explosions and Dynamics of Reactive Systems, I and II

J. R. Bowen, J. C. Leyer, and R. I. Soloukhin, editors

Companion volumes, *Dynamics of Explosions* and *Dynamics of Reactive Systems, I and II*, cover new findings in the gasdynamics of flows associated with exothermic processing—the essential feature of detonation waves—and other, associated phenomena.

Dynamics of Explosions (volume 106) primarily concerns the interrelationship between the rate processes of energy deposition in a compressible medium and the concurrent nonsteady flow as it typically occurs in explosion phenomena. *Dynamics of Reactive Systems* (Volume 105, parts I and II) spans a broader area, encompassing the processes coupling the dynamics of fluid flow and molecular transformations in reactive media, occurring in any combustion system. The two volumes, in addition to embracing the usual topics of explosions, detonations, shock phenomena, and reactive flow, treat gasdynamic aspects of nonsteady flow in combustion, and the effects of turbulence and diagnostic techniques used to study combustion phenomena.

Dynamics of Explosions
1986 664 pp. illus., Hardback
ISBN 0-930403-15-0
AIAA Members \$49.95
Nonmembers \$84.95
Order Number V-106

Dynamics of Reactive Systems I and II
1986 900 pp. (2 vols.), illus. Hardback
ISBN 0-930403-14-2
AIAA Members \$79.95
Nonmembers \$125.00
Order Number V-105

TO ORDER: Write AIAA Order Department, 370 L'Enfant Promenade, S.W., Washington, DC 20024. Please include postage and handling fee of \$4.50 with all orders. California and D.C. residents must add 6% sales tax. All orders under \$50.00 must be prepaid. All foreign orders must be prepaid. Please allow 4-6 weeks for delivery. Prices are subject to change without notice.